

Inclusive lepton production from heavy-hadron decay in pp collisions at the LHC.

Paolo Bolzoni* and Gustav Kramer†

*II. Institut für Theoretische Physik, Universität Hamburg,
Luruper Chaussee 149, 22761 Hamburg, Germany*

(Dated: October 31, 2018)

Abstract

We present predictions for the inclusive production of leptons (e^\pm, μ^\pm) originating from charm and bottom-hadrons at the CERN LHC in the general-mass variable-flavor-number scheme at next-to-leading order. Detailed numerical results are compared to data of the CMS, ATLAS and ALICE collaborations.

PACS numbers: 12.38.Bx, 13.85.Ni, 13.87.Fh, 14.40.Lb

arXiv:1212.4356v2 [hep-ph] 9 Apr 2013

*Electronic address: paolo.bolzoni@desy.de

†Electronic address: gustav.kramer@desy.de

I. INTRODUCTION

The investigation of heavy flavour (charm or bottom) production in proton-proton collisions at the LHC (Large Hadron Collider) are important for testing perturbative QCD calculations in a new energy domain, where very small Bjorken- x momentum fractions are expected to be probed. The detection of the heavy hadrons containing charm or bottom quarks can be done in several ways, either through their non-leptonic weak decays or through their semileptonic decays, where electrons or muons are measured inclusively.

Already at the RHIC (Relativistic Heavy Ion Collider), the PHENIX and STAR Collaboration [1, 2] measured the production of muons and electrons from heavy flavour decays in pp collisions at $\sqrt{S} = 0.2$ TeV. These data have been compared with perturbative QCD calculations in the FONLL framework [3, 4] and were found in agreement with the measurements within the experimental and theoretical uncertainties.

Experimentally the measurement of the semileptonic cross sections suffers from a large background due to the semileptonic decay of primary light hadrons including pions and kaons (the main contribution) and other meson and baryon decays (such as J/ψ and low mass resonances η , ρ , ω and ϕ), from secondary leptons produced from secondary light hadron decays, and from secondary hadrons escaping from material surrounding the tracking chambers. All these backgrounds must be subtracted based on Monte Carlo simulations using the usual event generators to obtain the semileptonic yield due to the decay of heavy hadrons.

The measured cross sections for the inclusive production of leptons from heavy hadron decays are of two types. In two experiments the production cross section is measured separately for solely b -hadron decays [5, 6]. In the CMS experiment [5] the b -hadron cross section was discriminated by measuring the muon transverse momentum with respect to the closest jet. In the ALICE experiment [6] the production cross section of electrons, $(e^+ + e^-)/2$ from semileptonic bottom hadron decays was selected by using the information on the distance of the secondary decay vertex with respect to the primary vertex. Due to their long lifetime bottom hadrons decay at a secondary vertex displaced in space from the primary collision vertex. In all other measurements of the semileptonic production which were presented by the ATLAS [7] and ALICE [8–10] collaborations no attempt was made to separate leptons from charm and bottom hadrons. Therefore these cross sections constitute

the sum of lepton (electrons or muons) production cross sections of all charmed hadrons (D^0, D^+, D_s and c -baryons) and all bottom hadrons (B^0, B^+, B_s and b -baryons).

At LHC energies the cross sections of charm and bottom production using special non-leptonic decays of charm and bottom hadrons have been reported. So, ALICE [11], ATLAS [12] and LHCb [13] presented cross section data on D^0, D^+, D^{*+} and D_s production and CMS [14] published measurements for B^+, B^0, B_s and Λ_b production cross sections. All these cross sections have been calculated in the framework of the general-mass-variable-flavour-number-scheme (GM-VFNS) [15], which has been developed in the last ten years for various processes. In this scheme we calculated the inclusive B meson production cross section in $p\bar{p}$ collision [16] at $\sqrt{S} = 1.96$ TeV and in pp collisions [17] and found good agreement with the respective data from the CDF run II [18] and also with the data from the CMS collaboration [14] at the LHC at $\sqrt{S} = 7$ TeV. Besides the data based on special non-leptonic decays of B mesons mentioned above there exist also several cross section measurements for $p\bar{p} \rightarrow BX$ and $pp \rightarrow BX$ followed by the inclusive decays $B \rightarrow J/\psi X$ and $B \rightarrow \psi(2S)X$. These cross sections have been calculated recently also in the GM-VFNS [19] and compared with experimental data from CDF [18, 20], CMS [21], LHCb [22], ATLAS [23] and ALICE [24] collaborations at the LHC. The agreement between the calculated cross sections and the data was satisfactory. In the same scheme the inclusive production of charmed mesons D^0, D^+, D^{*+}, D_s and the charmed baryon Λ_c has been calculated and the results for the ALICE [11], ATLAS [12] and LHCb [13] kinematic conditions have been presented in ref. [25] and compared to the experimental data in the respective presentations of the ALICE [11], ATLAS [12] and LHCb [13] collaborations and for the ALICE data also in [25].

The GM-VFNS is similar to the zero-mass variable-flavour-number scheme (ZM-VFNS), in which the heavy quark mass m is neglected in the calculation of the hard-scattering cross sections. The predictions in the ZM-VFNS are expected to be reliable only in the region of very large values of the transverse momentum p_T of the produced heavy hadron since terms of the order of m^2/p_T^2 are neglected in the hard-scattering cross sections. In the GM-VFNS these m^2/p_T^2 terms are retained as they appear in the so-called fixed-flavour-number scheme (FFNS) in such a way that by applying appropriate subtractions to the FFNS the GM-VFNS approaches the ZM-VFNS with the usual \overline{MS} prescription in the limit $p_T/m \rightarrow \infty$. Whereas in the FFNS the gluon and the light partons are the only active partons in the initial state and the heavy quark appears only in the final state, produced in the hard-scattering

process of light partons, in the GM-VFNS as in the ZM-VFNS, due to the subtraction of the mass-singular contributions in the initial and final state, the heavy quark appears also in the initial state, and for the final state appropriate fragmentation functions (FFs) for the transition *heavy – quark* \rightarrow *heavy – hadron* must be introduced which absorb the collinear singular contributions in the final state. Such FFs for the transitions $b \rightarrow B$, $b, c \rightarrow D^0$, D^+ and D^{*+} and $b, c \rightarrow D_s$ and Λ_c have been extracted in ref. [16, 26, 27] at NLO in the \overline{MS} factorization scheme with $n_f = 5$ (for b) and with $n_F = 4$ (for c) flavours, consistently within the GM-VFN framework using data for the scaled energy (x) distribution $d\sigma/dx$ of $e^+e^- \rightarrow BX$ and $e^+e^- \rightarrow DX$ etc, respectively, measured by the CERN LEP1, SLAC SLC, CESR CLEO and the KEKB Belle collaborations.

The content of this paper is as follows. In Sec. 2 we summarize our input choices of PDFs and B- and D-meson FFs. In this section we also explain how the fragmentation of these mesons into leptons has been calculated. In Sec. 3 we compare the predictions of the GM-VFN scheme with the existing data from the recent LHC run at $\sqrt{S} = 7$ TeV [5–10] and $\sqrt{S} = 2.76$ TeV [9]. We end with a summary in Sec. 4.

II. SETUP, INPUT PDFS AND FFs

The theoretical framework and results of the GM-VFN approach for $p\bar{p}$ (pp) collisions have been previously represented in detail in refs. [15, 16]. Here, we describe our choice of input for the numerical analysis for inclusive lepton (e or μ) production from charm and bottom hadrons. We use for the ingoing protons the PDF set CTEQ 6.6 [28] as implemented in the LHAPDF [29] library. This PDF set was obtained in the framework of a general-mass scheme using the input mass values $m_c = 1.3$ GeV, and $m_b = 4.5$ GeV, and for the QCD coupling $\alpha_s^{(5)}(m_Z) = 0.118$. The c - and b -quark PDFs have the starting scales $\mu_0 = m_c$ and $\mu_0 = m_b$, respectively.

The nonperturbative FFs for the transition of $b \rightarrow B$ were obtained by a fit to e^+e^- annihilation data from the ALEPH [30], OPAL [31] and SLD [32] collaborations and have been presented in [16]. The combined fit to the three data sets was performed using the NLO scale parameter $\Lambda_{\overline{MS}}^{(5)} = 227$ MeV corresponding to $\alpha_s^{(5)}(m_Z) = 0.1181$ adopted from ref. [28]. Consistent with the chosen PDFs, the starting scale of the $b \rightarrow B$ FF was assumed to be $\mu_0 = m_b$, while the $q, g \rightarrow B$ FFs, where q denotes the light quarks including the charm

quark, were taken to vanish at μ_0 . As input we used the FFs with a simple power ansatz which gave the best fit to the experimental data. The data from OPAL and SLD included all b -hadron final states, i.e. all B mesons, B^+ , B^0 and B_s and b -baryons while in the ALEPH analysis only final states with identified B^+ (B^-) and B^0 (\bar{B}^0) were taken into account. For the fit in ref. [16] it was assumed that the FFs of all b -hadrons have the same shape. This will also be assumed in this calculation. In addition we assumed that all b -hadrons have the same branching fractions and decay distributions into leptons as one of the B mesons, B^+ or B^0 . The only difference results from the different fractions $b \rightarrow b - hadron$, which are taken from the Particle Data Group [33]. Based on these values the prediction, for example for B^0 , is multiplied by 2.49, corresponding to leptons coming from B^0, B^+, B_s and Λ_b . The bottom mass in the hard scattering cross sections is $m_b = 4.5$ GeV as it is used in the PDF CTEQ6.6 and in the FFs for $b \rightarrow B$ etc.

For the transitions $c \rightarrow D^0, D^+$ we employ the FFs determined in [26]. They are based on fits to the most precise data on D meson production from the CLEO Collaboration at CESR [34] and from the Belle Collaboration at KEKB [35]. Actually there are several alternative fits presented in [26]. Here we use the so-called Global-GM fit, which includes fitting in addition to OPAL data [36] together with the CLEO and Belle results. The fits in [26] are based on the charm mass $m_c = 1.5$ GeV, which is slightly larger than the one used in the CTEQ6.6 PDF fits. The starting scale for $c \rightarrow D$ is $\mu_0 = m_c$ as it is for the $g, q \rightarrow D$ FFs, whereas for the $b \rightarrow D$ FF it is $\mu_0 = m_b$.

The subtractions related to renormalization and to the factorization of initial- and final-state singularities require the introduction of scale parameters μ_R, μ_I and μ_F . We choose the scales to be of order m_T , where m_T is the transverse mass $m_T = \sqrt{p_T^2 + m^2}$ and $m = m_b$ for the case of bottom quark production and $m = m_c$ for charm quark production. For exploiting the freedom in the choice of scales we introduce the scale parameters ξ_i ($i=R, I, F$) by setting $\mu_i = \xi_i m_T$. To describe the theoretical uncertainties we vary the values of ξ_i independently by factors of two up and down while keeping any ratio of the ξ_i parameters smaller than or equal to two. The uncertainties due to scale variation are the dominating source of theoretical uncertainties. Therefore PDF related uncertainties and variations of the bottom and charm mass are not considered.

The fragmentation of the final state partons i into lepton l ($l = e^\pm$ or μ^\pm) is calculated

from the convolution

$$D_{i \rightarrow l}(x, \mu_F) = \int_x^1 \frac{dz}{z} D_{i \rightarrow B}\left(\frac{x}{z}, \mu_F\right) \frac{1}{\Gamma_B} \frac{d\Gamma}{dz}(z, P_B). \quad (1)$$

In this formula $D_{i \rightarrow B}(x, \mu_F)$ is the nonperturbative FF determined in [16] for the transition $i \rightarrow B$ and in [26] for $i \rightarrow D$ (with subscript B replaced by D in (1)), Γ_B is the total B decay width ($\Gamma_B \rightarrow \Gamma_D$ in case of $i \rightarrow D$) and $d\Gamma(z, P_B)/dz$ is the decay spectrum of $B \rightarrow l$ or $D \rightarrow l$, respectively. For given lepton transverse momentum p_T and rapidity y , P_B is given by $P_B = |\mathbf{P}_B| = p_T \sqrt{1 + \sinh^2 y}/z$. The decay distribution $d\Gamma/dk'_L$, where the momentum k'_L is parallel to \mathbf{P}_B , is obtained from the decay distribution in the rest system of the B meson using the formula (3.16) in ref. [37], where this formula was derived for the decay $B \rightarrow J/\psi$ instead of $B \rightarrow l$. This leads to $d\Gamma(z, P_B)/dz$ used in eq.(1) with $z = k'_L/P_B$.

The electron energy spectrum in inclusive $B \rightarrow e\nu X$ decays has been measured by the BABAR Collaboration [38] in the range $E_e > 0.6$ GeV up to its kinematical limit. This spectrum has been measured at the $\Upsilon(4S)$ resonance. The partial branching fraction for $E_e > 0.6$ GeV has been determined as $\mathcal{B}[B \rightarrow e\nu X, E_e > 0.6 \text{ GeV}] = [10.36 \pm 0.06(\text{stat}) \pm 0.23(\text{syst})]\%$

Following an ansatz for the momentum spectrum as a function of p in GeV as given in ref. [39] we fitted the BABAR spectrum in the B rest system using the formula (3.9) in [37] for the transformation of the spectrum in the B rest system to the BABAR laboratory frame, where $|\mathbf{P}_B| = 0.341$ GeV by the following formula

$$f_B(p) = (-24.23 + 14711.2 \exp[-1.73 \ln^2[2.74 - 1.10p]]) \quad (2)$$

$$(-41.79 + 42.78 \exp[-0.5(\sqrt{(p - 1.27)^2}/1.8)^{8.78}])$$

This differs from the fit in [39] which was done in the BABAR $\Upsilon(4S)$ laboratory frame. $f_B(p)$ is related to the partial semileptonic decay spectrum $d\Gamma/dp$ by $d\Gamma/dp = cf_B(p)$ with $c = 4.27151 \cdot 10^{-6}$ according to [37], where $d\Gamma/dp$ has units $[ps^{-1}GeV^{-1}]$. The quality of the fit can be seen in Fig. 1 (left figure) together with the effect of the boost into the B rest system, which indeed is small. This fit yields for the partial branching fractions $\mathcal{B}(B \rightarrow e\nu X, p > 0.6 \text{ GeV}) = 11.04\%$ and $\mathcal{B}(B \rightarrow e\nu X, p > 0) = 12.35\%$. The latter branching fraction agrees approximately with the more recent PDG value $\mathcal{B}(B \rightarrow e\nu X, p > 0) = [10.74 \pm 0.16]\%$ [33].

The inclusive electron spectra for the decays $D^+ \rightarrow e^+\nu X$ and $D^0 \rightarrow e^+\nu X$ have been measured by the CLEO Collaboration [39] on the $\psi(3770)$ resonance ($\sqrt{S} = 3.73$ GeV)

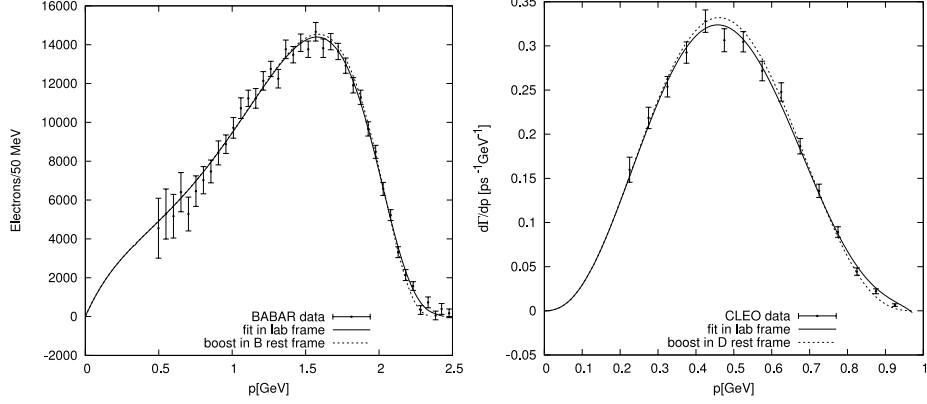


FIG. 1: Fit for inclusive lepton spectrum of B decays to BABAR (left frame) data in the BABAR laboratory frame together with spectrum boosted to the B rest frame and to inclusive lepton spectrum of D decays to CLEO (right frame) data in the CLEO laboratory frame together with the spectrum boosted to the D rest frame.

as a function of the electron momentum p . The measured partial branching fractions for $p > 0.2$ GeV are $\mathcal{B}(D^+ \rightarrow e^+\nu X, p > 0.2 \text{ GeV}) = [14.97 \pm 0.19(stat) \pm 0.27(syst)]\%$ and $\mathcal{B}(D^0 \rightarrow e\nu X, p > 0.2 \text{ GeV}) = [5.97 \pm 0.15(stat) \pm 0.10(syst)]\%$ from which, on the basis of fits to both spectra by the CLEO Collaboration, the following branching fractions $\mathcal{B}(D^+ \rightarrow e^+\nu X, p > 0) = [16.13 \pm 0.20(stat) \pm 0.33(syst)]\%$ and $\mathcal{B}(D^0 \rightarrow e^+\nu X, p > 0) = [6.46 \pm 0.17(stat) \pm 0.13(syst)]\%$ result. The corresponding PDG values are: $\mathcal{B}(D^+ \rightarrow e^+\nu X) = [16.07 \pm 0.30]\%$ and $\mathcal{B}(D^0 \rightarrow e^+\nu X) = [6.49 \pm 0.11]\%$ [33], which agree very well with the CLEO values [40]. The spectra of D^+ and D^0 as measured by CLEO coincide very well inside errors in the measured p range $0.2 < p < 1$ GeV. In the CLEO laboratory system the D^+ momentum $|\mathbf{P}_D|$ is 0.243 GeV and the D^0 momentum is 0.277 GeV. These numbers are needed for the fits in the D^+ and D^0 rest systems. The result of the fit for the spectrum in the D rest system, for example for the D^+ it is

$$f_D(p) = 17.91(p + 0.0034)^{2.66}(0.98 - p)^{2.97} \quad (3)$$

$f_D(p)$ in eq.(3) is equal to the lepton spectrum $f_D(p) = d\Gamma/dp$ in units of $[ps^{-1}GeV^{-1}]$. The quality of the fit to the CLEO data is shown in Fig. 1 in the right frame together with the spectrum in the D rest system. As can be seen there the difference between the two spectra is really small. The branching ratio for this spectrum is: $\mathcal{B}(D^+ \rightarrow e^+\nu X) = 15.29\%$, which is sufficiently close to the values from CLEO given above. With these parametrizations of the

electron spectra in the B , respectively D , rest system, we calculated the lepton spectra $d\Gamma/dx$ in the moving system as function of $k'_L = xP_B$ (xP_D) where k'_L is the lepton momentum that is parallel to \mathbf{P}_B (\mathbf{P}_D) using eq.(3.17) in [37].

To simplify the calculation we applied for $d\Gamma/dx$ the asymptotic formula as given in [37], which is the approximation for $P_B \gg M_B$ ($P_D \gg M_D$), where M_B and M_D are the masses of the B and D meson, respectively. We calculated $d\Gamma/dx$ for various P_B and found that the exact formula differs from the asymptotic formula by less than 5% for $P_B = 10$ GeV. This is easily achieved even for the smaller p_T values of the leptons in our applications since $d\Gamma/dx$ is peaked at very small x , so that the average x is below 0.2 in the case of B decays and similarly for D decays. The calculation of the lepton spectra is based on the calculation of the cross section $d\sigma/dp_T$ for specific D meson as reported in Ref.[25]. In the lepton spectra, the leptons originate from all charmed mesons D^0, D^+, D_s and the charmed baryon Λ_c . To make the calculation easier we calculated the lepton spectra for just one flavour state, the D^0 , and included the other D mesons, D^+, D_s and the contributions of charmed baryons, as for example Λ_c , by an appropriate normalization factor. For D^0 this normalization factor is 2.294 and was calculated using a compilation of charm hadron production fractions by Lohrmann [41] (Table 3 of this reference) and the lepton branching fractions for D^0, D^+, D_s and Λ_c equal to 0.0646, 0.161, 0.065 and 0.045, respectively [33]. In case we would have based this normalization factor on D^+ production, the normalization factor would be slightly different. This difference is compensated by the different normalization of $c \rightarrow D^+$ and the different lepton branching ratio, which result in almost equal cross sections $d\sigma/dp_T$ for the production of leptons from charmed hadrons via D^0 or D^+ .

III. RESULTS AND COMPARISON WITH LHC DATA

In this section we collect our results for the cross sections $d\sigma/dp_T$ as a function of p_T for the various LHC experiments and compare them with the published data. We start with the results on inclusive b-hadron production with muons at $\sqrt{S} = 7$ TeV by the CMS Collaboration [5] and the ALICE Collaboration [6]. The CMS data are for the production of the sum of $\mu^+ + \mu^-$ in the range from $6 \leq p_T \leq 30$ GeV, and are integrated over the rapidity y in the region $-2.1 \leq y \leq 2.1$. The comparison between the GM-VFNS predictions and the experimental data is shown in Fig. 2. The data lie slightly above

the full default curve (default scale choice) and agree better with the prediction with the maximal scale choice. The ALICE cross section $d\sigma/dp_T$ [6] for the production of electrons and positrons $((e^+ + e^-)/2)$ from bottom hadron decays at $\sqrt{S} = 7$ TeV in the rapidity range $-0.8 \leq y \leq 0.8$ is measured for smaller $p_T \leq 8$ GeV. Our prediction in comparison with the ALICE data, is shown also in Fig. 2, where we included the data only for $p_T \geq 1.5$ GeV. The agreement between the data and the prediction is quite good. The data with their errors lie quite well inside the theoretical uncertainty band, although nearer to the upper prediction from the respective scale choice (dashed line) at the larger p_T values. We remark that in the two predictions in Fig. 2 we included also the contributions from $b \rightarrow D \rightarrow lepton$. The FFs needed for this contribution were taken from [26] (global fit). These contributions are very small, of the order of 1 to 2 % compared to $c \rightarrow D$ contribution, depending on p_T , and are not visible in the logarithmic plots in Fig. 2. The $b \rightarrow D$ contributions are also included in all the following predictions. Note the different form of the cross section in the right frame of Fig. 2: $d^2\sigma/(2\pi dp_T dy)$ is in accordance to the ALICE definition, *i.e.* the cross section $d\sigma/dp_T$ is divided by the y bin width $\Delta y = 1.6$. Finally we note that in general at low p_T , the scale variation of the cross section is rather large. Some predictions go down up to $p_T = 1$ GeV. In this region the scale variation is particularly enhanced and, due to the contribution of b quarks in the initial state and the choice of the default scale $\sqrt{p_T^2 + m_b^2}$, is not suppressed as in other approaches as for example MC@NLO [42] in which the small p_T predictions are obtained in the FFNS as in the FONLL approach [3, 4]. This is an implementation issue in the limit $p_T/m \rightarrow 0$. Further details in the GM-VFNS framework are discussed in Ref.[25].

Next we present our predictions for the ATLAS and ALICE kinematical conditions for the combined cross sections $d\sigma/dp_T$ for electron (or muon) production resulting from the sum of charmed and bottom hadron production for $\sqrt{S} = 7$ TeV and one results from ALICE for $\sqrt{S} = 2.76$ TeV. This latter measurement was done by the ALICE collaboration in order to have the reference pp cross section for their $PbPb$ measurements at the same energy. In general the contributions from D (B) decays dominate at small (large) p_T and are approximately equal at $p_T \simeq 4$ GeV. The ATLAS data [7] consist of three different measurements of $d\sigma/dp_T$: (i) for the production of electrons ($e^+ + e^-$) as a function of p_T for $7 \leq p_T \leq 26$ GeV integrated over the rapidity range $-2.0 \leq y \leq 2.0$ excluding the rapidity interval $1.37 \leq |y| \leq 1.52$, (ii) the production of muons ($\mu^+ + \mu^-$) in the same p_T and y

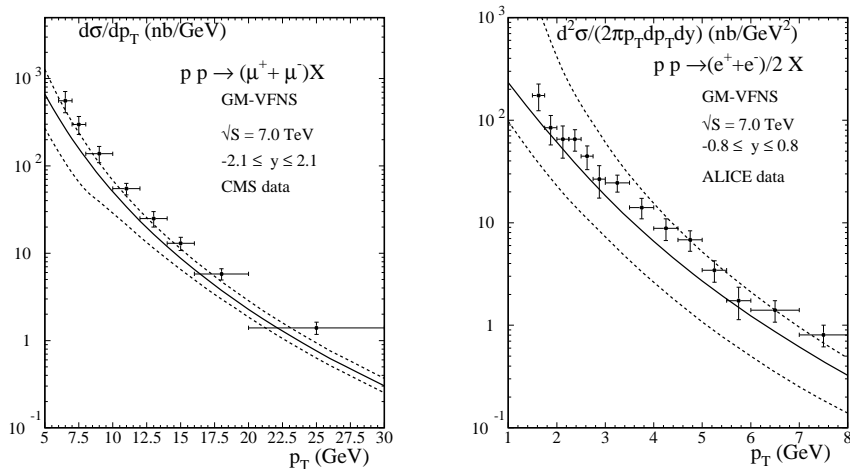


FIG. 2: GM-VFNS predictions for inclusive lepton production from bottom hadrons compared to CMS [5] and ALICE [6] data.

range as in (i), and (iii) the production of muons ($\mu^+ + \mu^-$) in the p_T range $4 \leq p_T \leq 100$ GeV and the y range $-2.5 \leq y \leq 2.5$. The result of our predictions is shown in Fig. 3. The agreement with the ATLAS data [7] is very good. The data points lie in all three plots with their errors inside the band obtained for the variation of the scale choices (upper and lower dashed curve). In the special plot for muon production (second ATLAS plot) the data lie very near to the default choice prediction (full curve) inside their small experimental errors. The same is true for the third plot in Fig. 3. Here the data and the default prediction agree even over a large p_T range, up to 100 GeV. This agreement in this large p_T range also shows that the evolution of the PDFs and FFs with increasing scale is very well accounted for by the data.

The second group of data comes from the ALICE collaboration. These are cross sections $d\sigma/dp_T$ for muon production at forward rapidity in the region $2.5 \leq y \leq 4.0$ at $\sqrt{S} = 7$ TeV [8] and at $\sqrt{S} = 2.76$ TeV [9]. The data for $d\sigma/dp_T$ are presented as a function of p_T between $2.0 \leq p_T \leq 12$ GeV, integrated over the total rapidity range and separately over five bins: (1) $2.5 \leq y \leq 2.8$, (2) $2.8 \leq y \leq 3.1$, (3) $3.1 \leq y \leq 3.4$, (4) $3.4 \leq y \leq 3.7$ and (5) $3.7 \leq y \leq 4.0$ as a function of p_T in the same transverse momentum range. The data and the comparison with our predictions are shown for the total y -range in Fig. 4 (second figure $\sqrt{S} = 2.76$ and third figure $\sqrt{S} = 7$ TeV) and for the cross sections integrated over the five y bins (1) to (5) in Fig. 4 (most right figure) and in Fig. 5. The agreement with the data

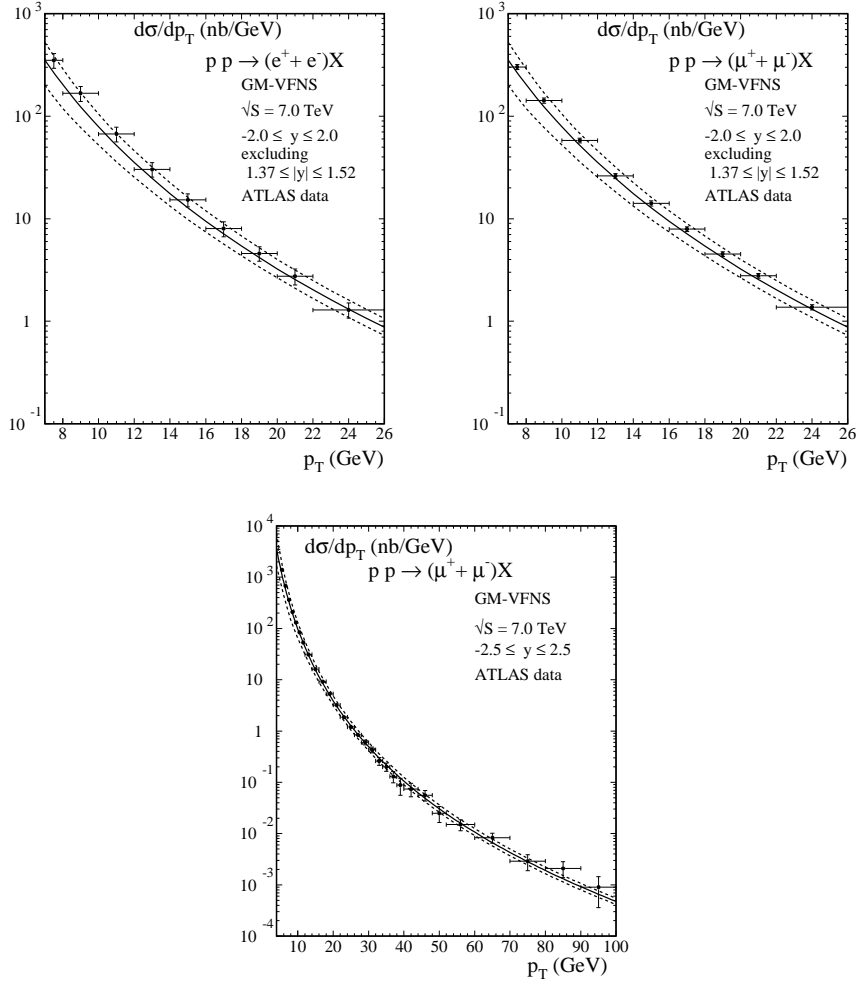


FIG. 3: GM-VFNS predictions for inclusive leptons from charm and bottom hadron decay compared to ATLAS [7] data.

is very satisfactory. The data points with their errors lie mostly between the curve for the default scale choice (full line) and the prediction for the maximal scale choice (upper dashed line). In addition we show in Fig. 4 also the results for the later published ALICE cross sections in the central rapidity region ($|y| \leq 0.5$) (most left figure). The agreement of the ALICE data [10] and our predictions with the default scale choice is again quite good.

IV. SUMMARY

We have calculated the cross sections for inclusive lepton production originating from heavy flavour decays at LHC c.m. energies of 2.76 and 7 TeV in the framework of GM-VFN

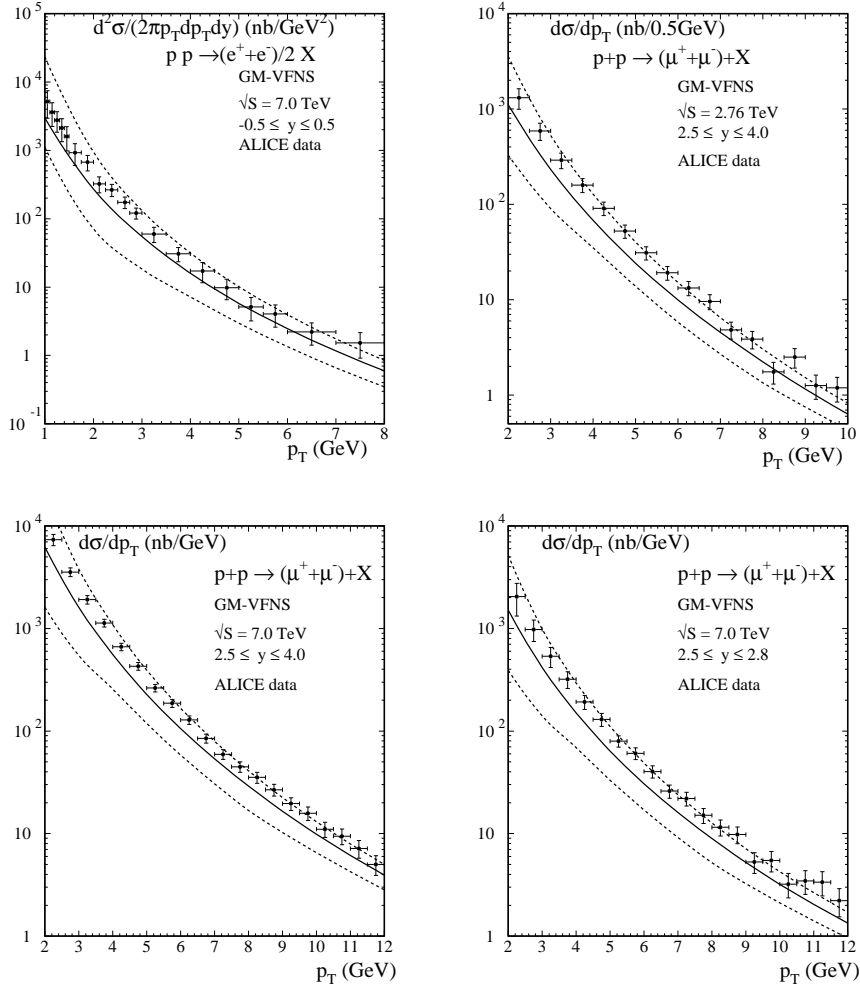


FIG. 4: GM-VFNS predictions for inclusive central and forward lepton production from the sum of charm and bottom hadron decay compared to ALICE [8–10] data.

scheme and compared them with measured cross sections $d\sigma/dp_T$ in different rapidity regions of the ALICE, ATLAS and CMS collaborations at the LHC. We found good agreement with all the experimental data inside the experimental and theoretical accuracies for both, the lepton data coming only from bottom hadron decays (CMS and ALICE data) and the lepton data for the sum of charm and bottom hadron decays. This shows that within the considered kinematical regions as given by the LHC collaborations the description of the inclusive production of charmed hadron and bottom hadron is well accounted for. Except the CMS data all other inclusive lepton production data from the LHC collaborations have been compared to predictions of the FONLL approach [3, 4] and similar good agreement between data and theoretical predictions has been found.

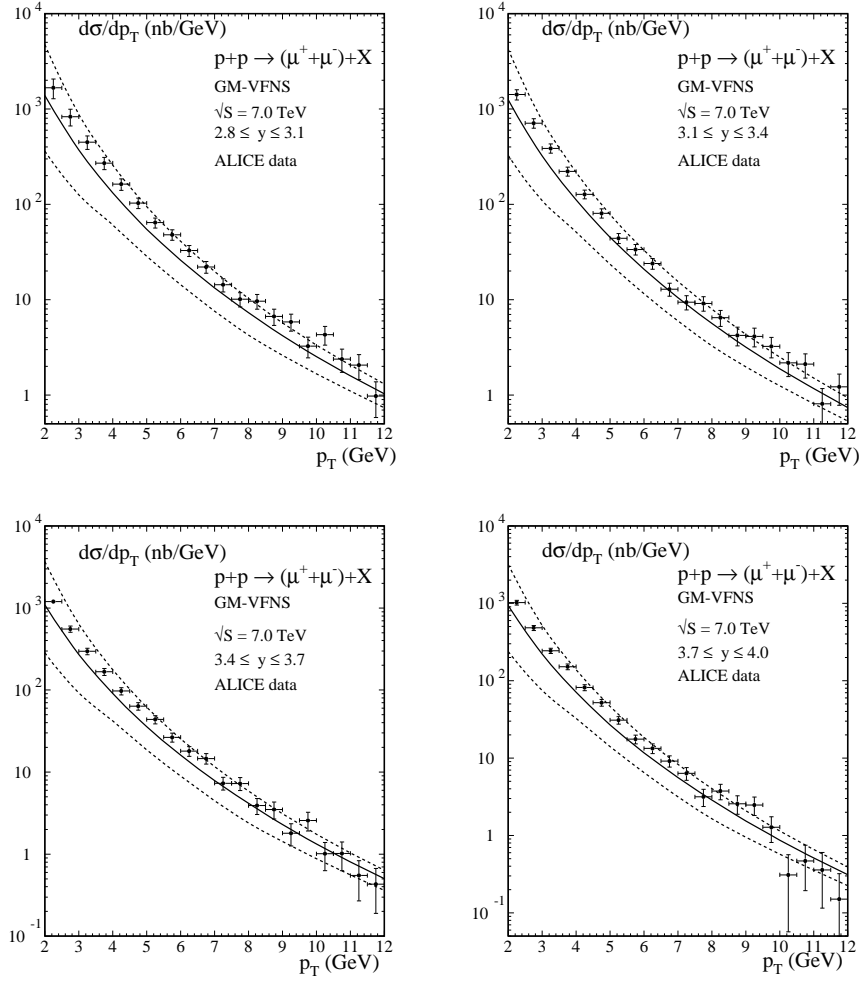


FIG. 5: GM-VFNS predictions for inclusive forward lepton production from charm and bottom hadron decay compared to ALICE [8] data in various rapidity regions.

Acknowledgments

We thank R. Maciula for sending us the data points of the BABAR collaboration. This work was supported in part by the German Federal Ministry for Education and Research BMBF through Grant No. 05 H12GUE, by the German Research Foundation DFG through Grant No. KN 365/7-1, and by the Helmholtz Association HGF through Grant No. Ha 101.

[1] S. S. Adler et al. (PHENIX Collaboration) Phys. Rev. Lett. 96, 032001 (2006); S. Adare et al. (PHENIX Collaboration) Phys. Rev. Lett. 97, 252002 (2006); S. S. Adler et al. (PHENIX

- Collaboration) Phys. Rev. D76, 092002 (2006); S. Adare et al. (PHENIX Collaboration) Phys. Rev. Lett. 103, 082002 (2009).
- [2] R. Abelev et al. (STAR Collaboration) Phys. Rev. Lett. 98, 192301 (2007); W. Xie, (STAR Collaboration) PoS DIS2010, 182 (2010).
- [3] M. Cacciari, P. Nason and R. Vogt, Phys. Rev. Lett. 95, 122001 (2005).
- [4] M. Cacciari, S. Frixione, N. Houdeau and M.L. Mangano, JHEP 1210, 137 (2012).
- [5] V. Khachatryan et al. (CMS Collaboration) JHEP 0311, 90 (2011).
- [6] B. Abelev et al. (ALICE Collaboration) arXiv:1208.1902 v1 [hep-ex].
- [7] G. Aad et al. (ATLAS Collaboration), Phys. Lett. B707, 438 (2012).
- [8] B. Abelev et al. (ALICE Collaboration), Phys. Lett. B708, 265 (2012).
- [9] B. Abelev et al. (ALICE Collaboration), Phys. Rev. Lett. 109, 112301 (2012).
- [10] B. Abelev et al. (ALICE Collaboration), Phys. Rev. D86, 112007 (2012).
- [11] B. Abelev et al. (ALICE Collaboration), JHEP 1201, 128 (2012).
- [12] The ATLAS Collaboration, ATL-PHYS-PUB-2011-012.
- [13] The LHCb collaboration LHCb-CONF-2010-013.
- [14] V. Khachatryan et al. (CMS Collaboratin) Phys. Rev. Lett. 106, 112011 (2011).
S. Chatrchyan et al. (CMS Collaboration) Phys. Rev. Lett. 106, 252001 (2011); Phys. Rev. D84, 052008 (2011); Phys. Lett. B714, 136 (2012).
- [15] B. A. Kniehl, G. Kramer, I. Schienbein and H. Spiesberger, Phys. Rev. D71, 014018 (2005); Eur. Phys. J. C41, 199 (2005).
- [16] B. A. Kniehl, G. Kramer, I. Schienbein and H. Spiesberger, Phys. Rev. D77, 014011 (2008).
- [17] B. A. Kniehl, G. Kramer, I. Schienbein and H. Speisberger, Phys. Rev. D84, 094026 (2011).
- [18] D. Acosta et al. (CDF Collaboration), Phys. Rev. D71, 032011 (2005); A. Abulencia et al. (CDF Collaboration) Phys. Rev. D75, 012010 (2007); T. Aaltonenet al. (CDF Collaboration) Phys. Rev. D79, 092003 (2009).
- [19] P. Bolzoni, B. A. Kniehl and G. Kramer (to be published)
- [20] T. Aaltonen et al. (CDF Collaboration), Phys. Rev. D80, 031103 R (2009).
- [21] S. Chatrchyan et al. (CMS Collaboration) JHEP 1102, 011 (2011).
- [22] R. Aaij et al. (LHCb Collaboration) Eur. Phys. J. C71, 1645 (2011).
- [23] G. Aad et al. (ATLAS Collaboration) Nucl. Phys. B850, 387 (2011).
- [24] B. Abelev et al. (ALICE Collaboration) JHEP 1211 (2012) 065.

- [25] B. A. Kniehl, G. Kramer, I. Schienbein and H. Spiesberger, *Eur. Phys. J.* C72, 2082 (2012).
- [26] T. Kneesch, B. A. Kniehl, G. Kramer and I. Schienbein, *Nucl. Phys. B* 799, 34 (2008).
- [27] B. A. Kniehl and G. Kramer, *Phys. Rev. D*74, 037502 (2006).
- [28] P. M. Nadolsky et al. (CTEQ Collaboration) *Phys. Rev. D*78, 013004 (2008).
- [29] LHAPDF, the les Houches Accord PDF Interface, URL:<http://projets.hepforge.org/lhapdf/pdfsets>.
- [30] A. Heister et al. (ALEPH Collaboration), *Phys. Lett.* B512, 32 (2003).
- [31] G. Abbiendi et al. (OPAL Collaboration), *Eur. Phys. J.* C29, 463 (2003).
- [32] K. Abe et al. (SLD Collaboration), *Phys. Rev. Lett.* 84, 4300 (2000); *Phys. Rev. D*65, 092006 (2002), 079905 (E) (2002).
- [33] K. Nakamura et al. (Particle Data Group) *J. Phys.* G37, 032002 (2010).
- [34] M. Artuso et al. (CLEO Collaboration) *Phys. Rev. D*70, 112001 (2004).
- [35] R. Seuster et al. (Belle Collaboration) *Phys. Rev. D*73, 032002 (2006)
- [36] G. Alexander et al. (OPAL Collaboration) *Z. Phys.* C72, 1 (1996).
- [37] B. A. Kniehl and G. Kramer, *Phys. Rev. D*60, 014006 (1999).
- [38] B. Aubert et al. (BABAR Collaboration), *Phys. Rev. D*69, 111104 R (2004).
- [39] M. Luszczak, R. Maciula and A. Szczurek, *Phys. Rev. D*79, 034009 (2009).
- [40] N. E. Adam (CLEO Collaboration) *Phys. Rev. Lett.* 97, 251801 (2006).
- [41] E. Lohrmann, arXiv:1112.3757 [hep-ex] 16 Dec 2011.
- [42] S. Frixione and B. R. Webber, *JHEP* 0206 (2002) 029.